

Deciphering the AMS cosmic-ray positron flux

A. De Rújula^{a,b}

^a*Instituto de Física Teórica (UAM/CSIC), Univ. Autónoma de Madrid, Spain;*

^b*Theory Division, CERN, CH 1211 Geneva 23, Switzerland*

(Dated: September 5, 2019)

The flux of cosmic-ray high-energy positrons has recently been measured by AMS with unprecedented precision. This flux is well above the expectation from secondary positrons made by the observed fluxes of nuclear cosmic rays impinging on the interstellar medium. Various authors have pointed out that the positron excess may originate at the primary cosmic-ray source itself, rather than in the more local ISM, thus avoiding the temptation to invoke a dark-matter decay or annihilation origin, or nearby pulsars. We investigate the possibility that the source is the one of a comprehensive model of gamma-ray bursts and cosmic rays, proposed two decades ago. The result, based on the original unmodified priors of the model –and with no fitting of parameters– very closely reproduces the shape and magnitude of the AMS observations.

PACS numbers: 98.70.Sa, 14.60.Cd, 97.60.Bw, 96.60.tk

I. INTRODUCTION AND OUTLOOK

The flux $F(E_+)$ of cosmic-ray (CR) positrons, measured by AMS, is shown as $E_+^3 F(E_+)$ in Fig.(1), copied here from [1]. In it the “Diffuse term” represents the contribution of CR protons and nuclei interacting with the matter of the interstellar medium (ISM) to produce secondary positrons. Concerning this term, the cited authors state: *Explicitly, we have chosen the first term of Eq. (4) based on the general trend of the commonly used cosmic ray propagation models, even though all have large uncertainties, but all show a maximum of the spectrum below 10 GeV.*

The “source” in “Source term” in Fig.(1) refers to the contention that the positron excess originates in the source of CRs. More or less conventional sources have been discussed by various authors [2].

In discussing quantitatively the “Source term” in Fig.(1) it is important to choose the diffuse term with heed. Lipari [3] has proposed a carefully built parametrization of the earlier AMS data [4]. It has two

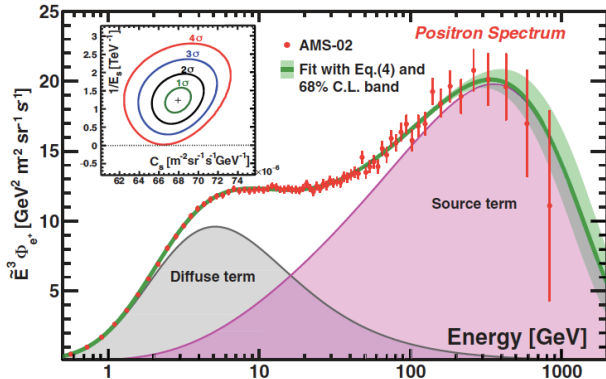


Figure 1: The AMS-02 positron spectrum [1] and its “diffuse” and “source” terms. The green line is their sum.

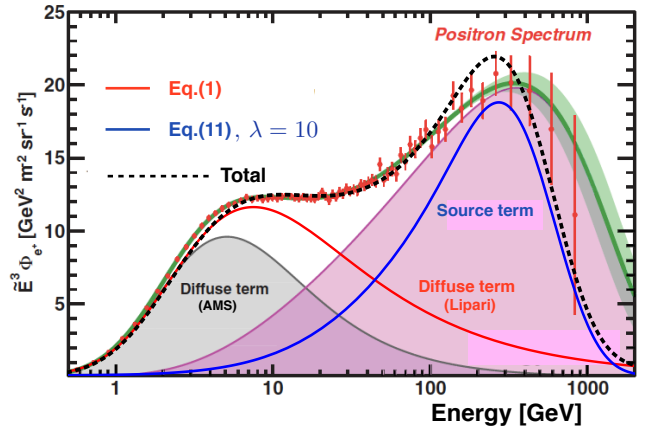


Figure 2: Our adopted diffuse term (red) and calculated source term (blue), and their sum (black, dashed).

terms, the second of which (the would-be source term) accounts for the observed change of spectral slope at $E_+ \simeq 20$ GeV. Without this contribution Lipari’s fit is:

$$\frac{d\Phi_{e^+}}{dE_+} = K \frac{E_+^2}{(E_+ + \epsilon)^2} \left[\frac{E_+ + \epsilon}{E_0} \right]^{-\Gamma} \quad (1)$$

with $K = 0.018/(\text{GeV m}^2 \text{sr})$, $\epsilon = 0.94$ GeV, $E_0 = 10$ GeV and $\Gamma = 3.62$. This will be the diffuse term adopted here. Multiplied by E_+^3 , it is shown as the red line in Fig.(2). The blue line in Fig.(2) is the source term we shall derive. Summed to the diffuse term it results in the black dotted line. The only arbitrarily chosen parameter in constructing this figure is the overall normalization of the source term. But, as we shall see, the calculated normalization is, in spite of inevitable uncertainties, remarkably compatible with the observed one.

II. THE MODEL

More than a decade ago a Cannon-Ball (CB) model of Gamma Ray Bursts (GRBs) and X-Ray Flashes (XRFs) was proposed [5] and elaborated [6]. The model is inspired by the observations of relativistic jets of matter emitted by quasars, and by microquasars such as GRS 1915+105 [7]. A-periodically, about once a month, this black hole launches two oppositely directed *cannonballs*, traveling at $v \sim 0.92c$. When this happens, the continuous X-ray emissions –attributed to an unstable accretion disk fed by a “donor” star– temporarily decrease.

The ‘cannon’ of the CB model is analogous to the ones of quasars and microquasars. In the core-collapse responsible for a stripped-envelope SNic event, due to the parent star’s rotation, a short-lived accretion disk is produced around the newly-born compact object.

A CB made of *ordinary-matter plasma* is emitted, as in microquasars, when part of the accretion disk falls abruptly onto the compact object. *Long-duration* GRBs are produced by these jetted CBs. The ‘*inverse*’ *Compton scattering* (ICS) of ambient light by the electrons within a CB produces a highly forward-collimated beam of higher-energy photons. Seen close to the CB’s direction of motion, the beam of γ -rays is a pulse of a GRB. Not so close, it is the pulse of an XRF. To agree with observations, CBs must be launched with typical Lorentz factors (LFs), $\gamma = \mathcal{O}(10^3)$, and baryon numbers, $N_B = \mathcal{O}(10^{50}) \sim 10^{-7} N_\odot$ [6].

The way the CB model describes the data and its many predictions regarding CRs and GRBs are summarized in the appendix of [8]. Comparisons with the “standard models” of GRBs are discussed in [9].

The CB model is also a model of primary non-solar CRs [10]. In that article, we argued that the model offers a very good description of the spectra and abundances of CR nuclei, and of electrons, with several priors chosen in their allowed ranges, but only one parameter to be fit to the data. The data have improved during the last decade. For example, measurements of the proton “knee” have been refined and knees in the He, Fe [11] and $e^+ + e^-$ [12] spectra have been observed, precisely as predicted by the CB model of CRs [8]. In a nutshell: CRs are made by CBs as they scatter the constituents of the ISM. The maximum energy of a CR of mass M is $2\gamma^2 M$, the limit of forward scattering. With the CBs’ LFs, γ , distributed around the typical value of $\mathcal{O}(10^3)$, the correspondingly gradual cutoff results in the correct positions and shapes of the cited knees [8].

III. THE CR e^+ SPECTRUM

A. The “wind”

The e^+ source flux of Fig.(2) is produced in the neighborhood of the CB-launching supernova (SN), as it traverses the SN’s close environment. Massive stars lose

Table I: Input priors of a CB and the SN’s “wind”.

Parameter	Value	Definition
γ	$\mathcal{O}(10^3)$	CB’s Lorentz factor ^{a, b}
N_B	10^{50}	CB’s baryon number ^a
c_s	$c/\sqrt{3}$	CB’s expansion velocity ^a
Σ	10^{16} g/cm	Wind’s surface density ^a

^a Typical CB-model value [6].

^b The γ distribution is that of [8], here Eq.(5).

mass in the form of “winds”, before they die in SN explosions. We shall refer to the pre-SN close-by material, accumulated by previous ejecta, as “the wind”, for short. As discussed in great detail in [6], the relevant observations [13, 14] indicate very high wind particle-number densities, $n \sim 5 \times 10^7 \text{ cm}^{-3}$, at the distances, $l = \mathcal{O}(10^{16})$ cm, of interest to the production of GRBs and positrons in the CB model. The measured n and mass density, ρ , decline roughly as $1/l^2$ and the wind’s “*surface density*” is $\Sigma \equiv \rho l^2 \sim 10^{16} \text{ g cm}^{-1}$ [13, 14].

The CB-model input priors are shown in Table I.

B. A CB sailing in the wind

In what follows, to avoid pedantic factors close to unity, we consider the composition of a CB (but not of the SN’s wind) to be that of hydrogen. At $\gamma = \mathcal{O}(10^3)$, the pp total cross section, $\sigma_{pp} \approx 40 \text{ mb}$, is dominantly inelastic. The p -nucleus cross section is an incoherent sum over the p -nucleon cross sections, with $\sigma_{pn} \approx \sigma_{pp}$. The CB’s radius of collisional transparency to the ambient protons or nuclei is $R_{pp} \sim [3 \sigma_{pp} N_B / (4\pi)]^{1/2} \sim 10^{12} \text{ cm}$, for $N_B = 10^{50}$. Since the CB’s initial internal radiation pressure is large, it should expand (in its rest frame) at a radial velocity $c_s = c/\sqrt{3}$, the speed of sound in a relativistic plasma. When the pp collisions cease the CB has travelled a distance $l_{max}(\gamma) = \sqrt{3} \gamma R_{pp} = 1.7 \times 10^{15} (\gamma/10^3) \text{ cm}$, where the LF reflects the relation between the times in the CB and SN rest systems.

What fraction of the CB’s protons is lost to interactions with the wind? Let the transverse radius of a CB at a distance l from the SN be $r_{CB}(l)$, corresponding to a surface $S(l) = \pi r_{CB}^2 = \pi l^2 / (3\gamma^2)$. The wind’s baryon-number density is $n(l) \approx \Sigma / (m_p l^2)$, with m_p the proton’s mass. The number of pp plus pn collisions (pN) is:

$$N_{pN} = \int_0^{l_{max}(\gamma)} S n dl = \frac{\pi R_{pp}}{\sqrt{3} \gamma} \frac{\Sigma}{m_p} = 1.1 \times 10^{49} \frac{10^3}{\gamma}, \quad (2)$$

so that a CB with $\gamma = 10^3$ would have lost $\sim 10\%$ of its $\sim 10^{50}$ protons to p -wind interactions. Kinematically, a negligible effect.

C. Surviving attenuation by the wind

The p -wind collisions give rise, mainly via the chain pp (or pn) $\rightarrow \pi$ or $K \rightarrow \mu^+ \rightarrow e^+$, to the source positrons of interest here. Not all positrons, however, manage to penetrate the SN's wind environment. Let $\sigma_T = 0.665 \times 10^{-24} \text{ cm}^2$ be the Thomson cross section, adequate for the study, quite independently of the nuclear target, of the penetrability of the wind to the γ -rays of a GRB [6]. Here we are interested in γ -rays or positrons of much higher energy, whose attenuation lengths by a pure-element intervening material are very similar, but decrease by an order of magnitude from H to Pb. We do not know the precise composition of the wind. In the wind of e.g. SN1997eg, H, He, N, O, Mg, Si and Fe lines have been observed [14]. We shall adopt, as a compromise or average, the γ -O or e^+ -O attenuation cross section which, above an energy of $\sim 1 \text{ GeV}$, is very close to constant and to σ_T [15].

Not all the positrons made in p -wind collisions escape unscathed to become observable: they may be re-absorbed by the wind's material. The probability that an e^+ produced at a distance l from the SN evades this fate, in a wind with a density profile $n_e \propto l^{-2}$, is $A(l) = \exp[-(l_{tr}^w/l)^2]$ with $l_{tr}^w = \sigma_T \Sigma/m_p$ the distance at which the remaining "optical" depth of the wind is unity.

Still referring to a single CB with $N_B = 10^{50}$ and LF γ , let us estimate the number, $N_{\rightarrow e}$, of proton-wind collisions whose produced positrons penetrate the wind unscathed. To do so, add an extra factor $A(l)$ to the integrand in Eq.(2)... and integrate. The result is:

$$N_{\rightarrow e}(\gamma) = \frac{\pi R_{pp}}{3\gamma^2} \frac{\Sigma}{m_p} I[l_{tr}^w, l_{max}(\gamma)],$$

$$I \equiv l_{max} \exp[-(l_{tr}^w/l_{max})^2] - \sqrt{\pi} \text{erfc}[l_{tr}^w/l_{max}]. \quad (3)$$

D. The e^+ energy distribution

Let $F(x, E_p)$, with $x \equiv E_+/E_p$, be the x distribution of positrons normalized (i.e. x -integrated) to their multiplicity at $E_p = \gamma m_p$. We shall use the $F(x, E_p)$ calculated in [16] and [17], which agree at the relevant $E_p = \mathcal{O}(\text{TeV})$, and are easy to check, since at such high energies the pp or $pn \rightarrow K, \pi$ yields approximately scale and all particles in the decay chain to positrons are approximately collinear. The simplest input to use are Eqs.(62 to 65) of [17], corrected by an –admittedly cosmetic– factor $\sim 5/6$ for the observed and expected primary charged-particle multiplicities in pp and pn collisions [18].

The number distribution of positrons as a function of their energy, once more referring to a single CB with

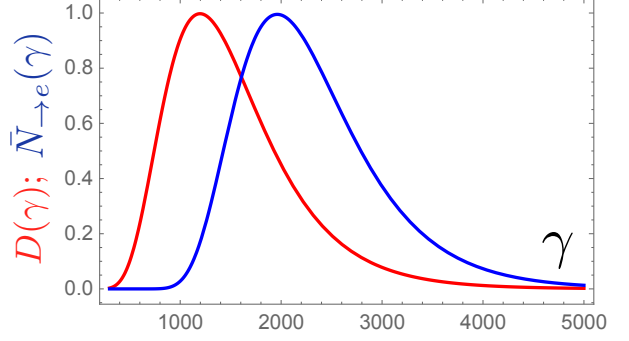


Figure 3: In red $D(\gamma)$. In blue $\bar{N}_{\rightarrow e}(\gamma)$. Both arbitrarily normalized in the figure.

$N_B = 10^{50}$ and LF γ , is:

$$\begin{aligned} \frac{dn(\gamma)}{dE_+} &= \int_0^1 dx F[x, m_p \gamma] N_{\rightarrow e}(\gamma) \delta(E_+ - m_p \gamma x) \\ &= \frac{1}{m_p \gamma} F\left[\frac{E_+}{m_p \gamma}, m_p \gamma\right] N_{\rightarrow e}(\gamma). \end{aligned} \quad (4)$$

E. The γ distribution of CBs

Next, we ought to weigh the above result with the distribution, $D(\gamma)$, of the Lorentz factors of CBs. We adopt the one that describes the CR proton knee and was used to predict [8] the shapes and positions of the He, Fe [11] and $e^+ + e^-$ [12] knees. To wit:

$$\begin{aligned} D(y) &= \exp(-[(y - y_0)/\sigma]^2); \\ y &\equiv \text{Log}_{10}[\gamma^2], \quad y_0 = 6.3, \quad \sigma = 0.5. \end{aligned} \quad (5)$$

The energy distribution of positrons made by a CB of $N_B = 10^{50}$, whose LF is randomly picked from the above distribution of CB's LFs is, *at the source*:

$$\frac{dN}{dE_+} = \int \tilde{D}(\gamma) \frac{dn(\gamma)}{dE_+} d\gamma, \quad (6)$$

with $dn(\gamma)/dE_+$ as in Eq.(4) and $\tilde{D} \equiv D/\int D d\gamma$.

Incidentally, the function $\bar{N}_{\rightarrow e} = \tilde{D} N_{\rightarrow e}$ is the number distribution of proton-wind collisions resulting in positrons that penetrate the wind, for a single CB of $N_B = 10^{50}$, and γ randomly picked from the distribution \tilde{D} . The shapes of $\tilde{D}(\gamma)$ and $\bar{N}_{\rightarrow e}(\gamma)$ are drawn in Fig.(3), showing how $\bar{N}_{\rightarrow e}(\gamma)$ is weighed to higher LFs than $D(\gamma)$ because larger- γ CBs keep interacting with the wind up to distances at which the latter is getting thinner.

F. The galactic rate of CB-emitting supernovae

Comparing the observed SN and long-duration GRB rates we concluded in [6] that *the GRB rate is consistent*

with being equal to the total rate of core-collapse SNe, or to a fraction of it that may be as small as $\sim 1/4$. It has been recently shown that at small redshifts, $z < 0.15$, the fraction of long duration GRBs without an associated bright SN is comparable to that of GRBs associated with SNe [19]. Crucial to these conclusions is the fact that in the CB model only a few per million GRBs are observable, since their ICS radiation is beamed within a cone of opening angle $\theta \sim 1/\gamma \sim 1$ mrad. Short GRBs, also emitting CBs in binary neutron star mergers [20], are only a fraction $\sim 7.35\%$ of the long ones [21]. Finally, a recent study confirms that the SN rate in the Galaxy is about two per century [22].

Abridging the previous paragraph into one number, we shall normalize the coming results to $N_{\text{Gal}}^{\text{SN}} = 1$, that is: one GRB-generating galactic SN per century. The observed median number of clear peaks (i.e. CBs) in long-duration GRB light curves is ~ 5 [23]. Since only “one-side” of a GRB is observable we set $N_{\text{CB}} = 10$, so that Eq.(6) must be multiplied by this number for one GRB-generating galactic SN.

IV. e^+ ESCAPE AND ENERGY LOSSES

Next we must take into account how the e^+ source spectrum of Eq.(6) is affected by energy losses in their interactions with the radiation and magnetic fields of the Galaxy, as well as their possible escape therefrom.

A. Positron escape

Let us first discuss the escape from the Galaxy, characterized by a confinement time:

$$\begin{aligned} \tau_{\text{conf}}(E_+) &= \tau_0 (1 \text{ GeV}/E_+)^{\beta_{\text{conf}}}; \\ \tau_0 &\sim 2.5 \times 10^7 \text{ years}, \beta_{\text{conf}} \sim 0.6, \end{aligned} \quad (7)$$

with τ_0 and β_{conf} estimated from observations of astrophysical and solar plasmas and corroborated by measurements of the relative abundances of secondary CR isotopes [24]. Recent measurements of the B/C ratio [25] imply, at low rigidity, R , smaller values of β_{conf} than given in Eq.(7), see Fig.(2) in [25]. But, as theoretically expected, $\beta_{\text{conf}}(R)$ flattens as R increases. The measured value at the highest-rigidity point ($R = 860$ GV) is $.52 \pm .13$. The rigidities of the positrons discussed here are similar. It is therefore reasonable, as we do in what follows, to adopt the “traditional” $\beta_{\text{conf}} = 0.6$, compatible with the results of [24] and [25]. The outcome for a more “theoretical” choice at relatively low E_+ , $\beta_{\text{conf}} = 1/3$ [26] is not significantly different.

B. Positron energy loss by ICS of starlight

The e^+ energy loss of positrons due to ICS on ambient light in the near-UV to near-IR regime requires a detailed

treatment [27], if only because it is the only energy-loss mechanism that might significantly affect the *shape* of the observed e^+ spectrum.

The energy density of the interstellar radiation field of the Galaxy, U , has been carefully modeled in [28, 29], allowing one to compare its local value, U_{loc} , some 7.5 kpc away from the galactic center, to its values, U_{in} , in the inner disk at 0 to 3 kpc from the center, the domain where most galactic SNe occur. At wavelengths from 0.1 to 10 μm –to which we shall refer to as “starlight”– the values of U_{in} are ~ 5 to ~ 30 times larger than U_{loc} . In this wavelength domain we shall adopt the value $U_{\text{in}} = 10 U_{\text{loc}}$, but compare the results with the ones for $U_{\text{in}} = U_{\text{loc}} \sim 0.39 \text{ eV/cm}^3$, to illustrate the sensitivity to this input. The values in the Far InfraRed (FIR) domain (wavelengths from 15 to $10^3 \mu\text{m}$) the difference between U_{in} and U_{loc} is less pronounced [28, 29].

The ICS of starlight by positrons in the energy domain we study brackets the transition from a Thomson to a Klein-Nishina cross section. In this respect we follow the analysis in [30] and [27]. Define an energy-loss time, τ_* :

$$\begin{aligned} \tau_*(E_+, \lambda) &= 3m_e^2/[4\sigma_T c E_+ U_*(E_+, \lambda)], \\ U_*(E_+, \lambda) &= \lambda U_{\text{loc}} E_{\text{KN}}^2/(E_{\text{KN}}^2 + E_+^2), \\ E_{\text{KN}} &= 0.27 (m_e c^2)^2/(kT), \end{aligned} \quad (8)$$

where λ is introduced to study varying the amount of starlight energy density in the inner Galaxy, and $E_{\text{KN}} = 140 \text{ GeV}$ for light at a temperature $T = 5700 \text{ K}$ [30].

C. Other e^+ energy losses and the combined lifetime

Three other sources affecting the local spectrum of positrons are their interactions with ambient photons of various types: the real ones of the Cosmic Background Radiation (CBR) and the FIR, and the virtual ones of magnetic fields (B) –ICS on the latter photons is usually called bremsstrahlung. Choose these photon energy-densities to be the locally measured ones ($U_{\text{B}}, U_{\text{FIR}}, U_{\text{CBR}} \sim (0.4, 0.4, 0.26) \text{ eV/cm}^3$ and define $U_{\text{soft}} = U_{\text{B}} + U_{\text{FIR}} + U_{\text{CBR}}$. The corresponding positron lifetime is:

$$\tau_{\text{soft}}(E_+) = 3m_e^2/[4\sigma_T c E_+ U_{\text{soft}}]. \quad (9)$$

To obtain the positron lifetime, τ , combining the effects of escape and the various energy-loss mechanisms, one inverts the sum of the inverse separate lifetimes:

$$\tau(E_+, \lambda) = \frac{1}{\tau_{\text{conf}}^{-1}(E_+) + \tau_*^{-1}(E_+, \lambda) + \tau_{\text{soft}}^{-1}(E_+)}. \quad (10)$$

The various lifetimes we have discussed are shown in Fig.(4). Notice the shapes of $\tau(E_+, 1)$ and $\tau(E_+, 10)$.

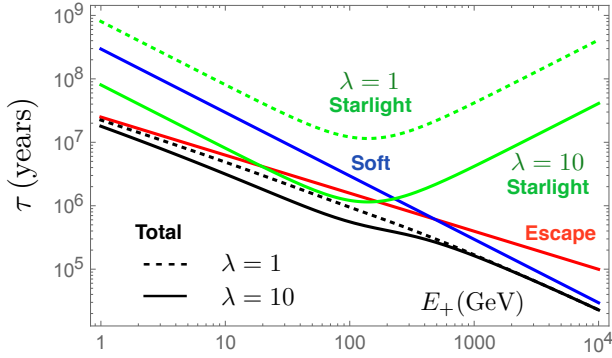


Figure 4: Positron lifetimes as functions of energy. The red “Escape” line is Eq.(7). The green lines are for the effect of starlight and two values of λ in Eq.(8). The blue “Soft” line is Eq.(9). The black “Total” lines are for two values of λ in Eq.(10).

V. THE LOCAL FLUX OF POSITRONS

To recapitulate and proceed, the number flux of Eq.(6), multiplied by $N_{CB}=10$ (the median number of CBs), by $N_{Gal}^{SN}=1/\text{century}$ (the galactic rate of CB-emitting SNe), and by the lifetime $\tau(E_+, \lambda)$ of Eq.(10) (expressed in centuries) is the predicted number flux per unit energy interval of the source positrons that will still be in the Galaxy and have an energy E_+ . To convert this result into a flux per stereo-radian and per unit surface, we must still multiply it by $c/(4\pi)$ and distribute the positrons over the Galaxy. One way of doing the latter is to use a state-of-the-art CR propagation code, such as GALPROP [31, 32] or DRAGON [33], in one of their many options. Instead we use a simpler procedure that conveys the gist of the argument. We do this in two steps:

In a first very rough estimate, assume the positrons to be uniformly distributed in a “leaky box” cylinder with the usually assumed dimensions: 15 kpc radius and 4 kpc (half-)height, that is $V=1.66 \times 10^{68} \text{ cm}^3$. The result for the e^+ flux F is then:

$$\frac{d\Phi_{e^+}(\lambda)}{dE_+} = N_{Gal}^{SN} N_{CB} \frac{dN}{dE_+} \tau(E_+, \lambda) \frac{c}{4\pi V}, \quad (11)$$

Second, we reinterpret this outcome by assuming that at our position in the Galaxy (half-way to the rim of the leaky box) the number density of positrons, which ought to decrease with distance to the galactic centre, is close to the above average. State-of-the art calculations not based on a leaky box support this claim. For instance, Fig.(19) of [34] or Fig.(6.8) of [35]. The latter figure is also for CR protons, not positrons, but is computed with “a Plain Diffusion setup” with DRAGON [33] (protons and positrons lose energy at different rates, but at relativistic energies they diffuse in the same manner).

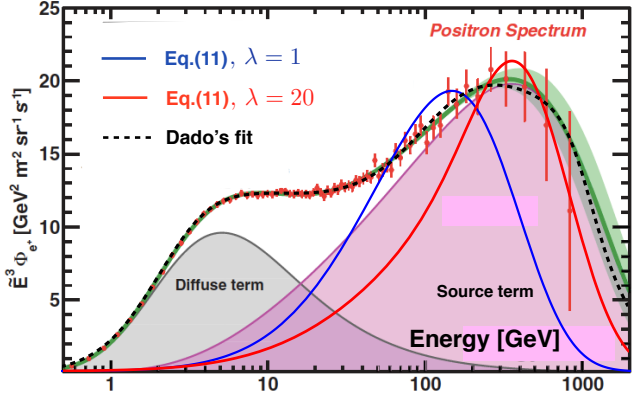


Figure 5: Sensitivity to various values of the parameters.

The result of Eq.(11), with $\lambda = 10$, and duly multiplied by E_+^3 , is the blue “source” term in Fig.(2)... but for the fact that the predicted normalization is 1.23 times larger.

The above result on the normalization is either an incredible coincidence or a very satisfactory consistency check, given the admittedly large number of accumulated uncertainties –a non-obvious (i.e., non-linear) example: an increase by 40% (or 19%) of the assumed wind surface density, Σ , would reduce the cited normalization by a factor of two (or 1/1.23).

VI. MINOR POINTS OF DISCUSSION

Regarding the shape of our source term, various comments are illustrated in Fig.(5). There, the blue curve is Eq.(11) with $\lambda = 1$, that is with the starlight energy density measured in the solar neighborhood. It is to be compared with the blue ($\lambda = 10$) result of Fig.(2), for which the Thomson to Klein-Nishina transition is more pronounced. The red curve in Fig.(5) has $\lambda = 20$ and a distribution of LFs, Eq.(5), centered at the same maximum, but slightly broader ($y_0 = 6.53$, $\sigma = 0.8$). A LF distribution enhanced a large γ in Eq.(6) is a way to compensate for the fact that the $F(x, E_p)$ inputs we have used [16, 17] lack positrons made in the decay chains of charmed particles. These positrons are relatively few, but more energetic than the ones from π and K decays.

It should be clear that one could obtain a perfect description of the data by fitting various parameters, such as λ and the energy density of magnetic fields and the FIR. This was done, with otherwise much less detail, in [36]. The black dashed curve in Fig.(5) is a fit (Shlomo Dado, private communication) with $\chi^2/(\text{dof})=0.58$ and 9 fitted parameters, including the ones describing the diffuse term. Providing a perfect fit may be esthetically satisfactory, but is not necessarily decisive since, after all, there are no undebatable results for the diffuse term’s size under the source term peak.

In the CB model the photons of a GRB pulse are made

by ICS of light by a CB's electrons and their typical number, integrated over energy and angles, is $N_{\text{GRB}}^{\gamma} = 5 \times 10^{52}$ [6]. Our source positrons are accompanied by γ -rays in slightly higher numbers and with a slightly harder spectrum [16, 17], forward collimated within an angle $\sim p_{\text{T}}/E$ close to the GRB photon's opening angle, $1/\gamma$. In an observed GRB, are these γ -rays of higher E than the typical $E_{\text{GRB}} = 250$ keV observable?

Alas, the answer is so negative that a rough estimate suffices. The ratio of γ -rays or e^{+} 's surviving wind absorption to the number of pp or pn collisions is $I/(\sqrt{3}\gamma)$, where Eqs.(2,3) have been used. At the maximum of $\bar{N}_{\rightarrow e}(\gamma)$ at $\gamma \sim 2000$ in Fig.(3) this ratio is $\sim 5\%$ of the number of pp or pn collisions at that same LF γ : 5×10^{48} according to Eq.(2). All in all the number of prompt hard photons per GRB pulse is $\sim 2.5 \times 10^{47}$, that is a miserable 5×10^{-6} of N_{GRB}^{γ} . Moreover their spectrum,

akin to the e^{+} one of Eq.(4), is strongly peaked at low energies, with only a small fraction above, say, 1 GeV.

VII. CONCLUSION

The CB model predicts the shape and normalization of the AMS positron spectrum in a very satisfactory way.

Acknowledgment: A. De Rújula acknowledges that this project has received funding/support from the European Union's Horizon 2020 research and innovation programme under the Marie Skłodowska-Curie grant agreement No 690575. I am particularly indebted to Shlomo Dado and Arnon Dar for discussions and advice.

-
- [1] M. Aguilar et al., Phys. Rev. Lett, **122**, 041102 (2019).
 - [2] S. Dado, & A. Dar, Mem. Soc. Ast. It. **81**, 132 (2010), arXiv:0903.0165; P. Blasi, Phys. Rev. Lett. **103**, 051104 (2009), arXiv:0903.2794; L. Stawarz, V. Petrosian, & R. D. Blandford, Astrophys. J. **710**, 236 (2010), arXiv:0908.1094; S. Dado, & A. Dar, arXiv:1505.04988.
 - [3] P. Lipari, arXiv:1810.03195v1.
 - [4] M. Aguilar et al., Phys. Rev. Lett. **113**, 121102 (2014).
 - [5] A. Dar & R. Plaga, Astron. & Astrophys. **349**, 259 (1999); A. Dar, A. De Rújula & N. Antoniou, Proc. Vulcano Workshop 1999 (eds. F. Giovannelli and G. Mannocchi) p. 51 Italian Physical Society, Bologna-Italy, astro-ph/9901004; A. De Rújula, Nucl. Phys. Proc. Suppl. **151** 23 (2006); hep-ph/0412094;
 - [6] A. Dar & A. De Rújula, Phys. Rept. **405**, 203, (2004), arXiv:astro-ph/0308248 and references therein.
 - [7] I.F. Mirabel & L.F. Rodriguez, Annu. Rev. Astron. Astrophys. **37**, 409 (1999).
 - [8] A. De Rújula, Phys. Lett. **B790C**, 444 (2019), arXiv:1802.06626, and references therein.
 - [9] A. Dar & S. Dado, arXiv:1810.03514.
 - [10] A. Dar and A. De Rújula, Phys. Rept. **466**, 179 (2008), hep-ph/0606199, and references therein.
 - [11] J.R. Hoerandel, Proc. of the *Workshop on Physics of the End of the Galactic Cosmic Ray Spectrum*, Aspen, USA, 2005, astro-ph/0508014.
 - [12] L. Accardo et al., Phys. Rev. Letters **113**, 121101 (2014); J.J. Beatty, J. Matthews, & S.P. Wakely in Review of Particle Properties. <http://pdg.lbl.gov/2017/reviews/rpp2017-rev-cosmic-rays.pdf>; DAMPE Collaboration, Nature **552**, 63 (2017). arXiv:1711.10981v1, and references therein; O. Adriani et al., Phys. Rev. Letters **120**, 261102 (2018); astro-ph/1806.09728.
 - [13] M. Turatto et al., ApJ, **534**, L57 (2000); A. Fassia, et al. MNRAS, **325**, 907 (2001); I. Salamañca, R. J. Terlevich, & G. Tenorio-Tagle, MNRAS, **330**, 844 (2002); N. N. Chugai & I. J. Danziger, 2003, Astron. Lett. **29**, 649 (2003), astro-ph/0306330.
 - [14] I. Salamañca, et al., MNRAS, **300**, L17S (1998).
 - [15] <https://physics.nist.gov/PhysRefData/Xcom/html/xcom1.html>
 - [16] I.V. Moskalenko & A.W. Strong, Astrophys. J. **493**, 694 (1998).
 - [17] S. R. Kelner, F. A. Aharonian, & V.V. Bugayov Phys. Rev. **D74**, 034018 (2006).
 - [18] J. F. Grosse-Oetringhaus & K. Reygiers J. Phys. G37:083001, (2010).
 - [19] S. Dado & A. Dar, ApJ, **855**, 88 (2018).
 - [20] S. Dado, A. Dar & A. De Rújula, arXiv:1712.09970.
 - [21] J. Greiner <http://www.mpe.mpg.de/~jcg/grbgen.html>
 - [22] R. Diehl et al. Nature **439**, 45 (2006).
 - [23] See, e.g., A. Lee, E. D. Bloom and J. Scargle in AIP Conf. Proc. **384**, no.1, 47 (1996).
 - [24] See, e.g. S.P. Swordy et al., Astrophys. J. **349**, 625 (1990).
 - [25] M. Aguilar et al., Phys. Rev. Lett. **117**, 231102 (2016).
 - [26] A. N. Kolmogorov, Dokl. Akad. Nauk SSSR **30**, 301 (1941); Proc. R. Soc. **A434**, 9 (1991).
 - [27] S. Dado & a. Dar, The Astrophysical Journal **812**, 38 (2015), arxiv.org/abs/1502.01244.
 - [28] T. A. Porter, & A. W. Strong, in *Proc. 29th Int. Cosmic Ray Conf. 2005* (Pune), astro-ph/0507119.
 - [29] T. A. Porter, I. V. Moskalenko & A. W. Strong or Astrophys. J. **648**, L29, (2006) , arXiv:astro-ph/0607344.
 - [30] R. Schlickeiser & Ruppel, J., New Journal of Physics, **12**, 033044 (2010).
 - [31] A. W. Strong & I. V. Moskalenko, Contribution to the 31st ICRC, Lodz, Poland, July 2009. Paper ID 0626, arXiv:0907.0565.
 - [32] GALPROP, <https://galprop.stanford.edu/>
 - [33] C. Evoli & al. JCAP **02**, 015 (2017), arXiv:1607.07886.
 - [34] A. W. Strong & I. V. Moskalenko in *Topics in Cosmic Ray Astrophysics* (vol. 230 in Horizons in World Physics), ed. M. A. DuVernois (New York: Nova Science Publishers), pp.81-103 (2000), arXiv:astro-ph/9812260
 - [35] D. Gaggero, in *Cosmic Ray Diffusion in the Galaxy and Diffuse Gamma Emission*, Springer Science & Business Media, Jul 9, 2012
 - [36] S. Dado & A. Dar, Journal of High Energy Physics, **9-10**, 9 (2016), arXiv:1504.03261.